



## Supporting Online Material for

### Asymmetric T Lymphocyte Division in the Initiation of Adaptive Immune Responses

John T. Chang, Vikram R. Palanivel, Ichiko Kinjyo, Felix Schambach, Andrew M. Intlekofer, Arnob Banerjee, Sarah A. Longworth, Kristine E. Vinup, Paul Mrass, Jane Oliaro, Nigel Killeen, Jordan S. Orange, Sarah M. Russell, Wolfgang Weninger, Steven L. Reiner\*

\*To whom correspondence should be addressed. E-mail: sreiner@mail.med.upenn.edu

Published 1 March 2007 on *Science* Express  
DOI: 10.1126/science.1139393

#### **This PDF file includes:**

Materials and Methods  
Figs. S1 to S8  
References

## Supporting online material

Material and Methods

Figs. S1-S8

References

## Materials and Methods

### Mice

All animal work was done in accordance with Institutional Animal Care and Use Guidelines of the University of Pennsylvania. Wild-type C57BL/6 and B10.D2 mice, C57BL/6 *Rag1*<sup>-/-</sup>, *Icam1*<sup>-/-</sup>, and P14 TCR transgenic mice recognizing LCMV peptide gp33-41/Db, as well as B10.D2 WT15 TCR transgenic mice recognizing the *Leishmania* peptide LACK156-173/I-Ad (SI) were housed in specific pathogen-free conditions prior to infectious challenges.

### Adoptive transfers and infectious challenges

For microscopy, CD8<sup>+</sup> and CD4<sup>+</sup> T cells were purified using subset-specific T Cell Isolation Kit (Miltenyi Biotec) from P14 and WT15 TCR transgenic mice, respectively.  $3 \times 10^6$  CFSE-labeled (Molecular Probes) CD8<sup>+</sup> and CD4<sup>+</sup> T cells were adoptively transferred i.v. into wild-type C57BL/6 or B10.D2 mice, respectively. Transgenic CD8<sup>+</sup> T cells were also transferred into C57BL/6 *Rag1*<sup>-/-</sup> and *Icam1*<sup>-/-</sup> mice. For CD8<sup>+</sup> T cell experiments, C57BL/6 wild-type and *Icam1*<sup>-/-</sup> recipients were infected i.v. 24h prior to T cell transfer with  $5 \times 10^3$  colony forming units (CFU) of recombinant *Listeria monocytogenes* expressing gp33-41 (gp33-*L. monocytogenes*, the generous gift of Hao Shen). *Rag1*<sup>-/-</sup> recipients were never experimentally infected. In preliminary experiments, it was determined that donor T cells from wild-type and *Icam1*<sup>-/-</sup> recipients did not divide or become activated over the course of any of the experimental intervals in the absence of pathogen challenge. For CD4<sup>+</sup> T cell experiments, wild-type B10.D2 mice were inoculated subcutaneously in the hind footpad 24h prior to T cell transfer with  $2 \times 10^6$  late stationary-phase *Leishmania major* promastigotes. At 32h after adoptive transfer of T cells, single cell suspensions of the spleen (for CD8<sup>+</sup>) and popliteal lymph node (for CD4<sup>+</sup>) were sorted using a FACS Aria (BD) to isolate undivided T cells (parental generation; brightest CFSE peak; 95% purity). For conjoined twin daughter cell experiments, sorted parent cells were cultured in media containing cytochalasin B (10 $\mu$ M) for 4h at 37C prior to fixation, staining, and confocal imaging. Owing to pre-transfer purification, parent cells were >90% CD8<sup>+</sup> and CD4<sup>+</sup>, respectively. Identical results were obtained using monoclonal P14 transgenic *Rag1*<sup>-/-</sup> donor T cells.

For analysis of daughter cells,  $10^7$  CFSE-labeled splenocytes from P14 TCR transgenic mice were transferred i.v. into C57BL/6 wild-type, *Rag1*<sup>-/-</sup>, and *Icam1*<sup>-/-</sup> mice. 24h after transfer, C57BL/6 wild-type and *Icam1*<sup>-/-</sup> recipients were infected i.v. with gp33-*L. monocytogenes*. At 48h after infection, single cell suspensions of the spleen were stained with the PE- and APC-conjugated mAbs against CD8, LFA-1 (CD11a), CD62L, CD69, CD43 (1B11), CD25, CD44, Granzyme B, and IFN $\gamma$ , and analyzed by flow cytometry. Fixation and permeabilization were used to detect intracellular Granzyme B and IFN $\gamma$ . For detection of IFN $\gamma$ , cells were stimulated ex vivo for 4h with PMA/Ionomycin. In some experiments, CD8<sup>+</sup> daughter T cells (second brightest CFSE peak) were sorted based on bimodality (higher and lower peak) among CD8<sup>+</sup> events.  $2 \times 10^3$  putative proximal (higher CD8) and distal (lower CD8) daughter cells from each

group were adoptively transferred i.v. into new naïve wild-type recipients. Either at the time of transfer or 30d later, recipient mice and untransferred controls were challenged with  $5 \times 10^3$  CFU gp33-*L. monocytogenes*. 4d after challenge, recipient mice were sacrificed and quantitative bacterial burdens in the spleens were determined. Briefly, spleens were homogenized in 1% Triton X (Roche), and serial dilutions plated on brain-heart infusion (Sigma) agar plates incubated overnight at 37C. P values were calculated using unpaired student *t*-test.

### Confocal microscopy

Cells were allowed to settle briefly on poly-L-lysine (Sigma) coated coverslips (Fisher Scientific). Cells were then fixed with 4% paraformaldehyde (Sigma), permeabilized with 0.3% Triton X (Roche), and blocked with 0.25% fish skin gelatin (Sigma) and 0.01% saponin (Sigma) in PBS. The following antibodies were used: mouse anti- $\beta$ -tubulin (Sigma); rat anti- $\alpha$ -tubulin (Abcam); rat anti-CD11a, rat anti-CD90-biotin, rat anti-IFN $\gamma$ R-biotin, rat anti-IFN $\gamma$ , rat anti-CD8-Alexa Fluor 647 (Pharmingen); rat anti-CD3, rat anti-CD8, hamster anti-CD3, rat anti-CD4 (Caltag); rabbit anti-Scribble, rabbit anti-Numb, rabbit anti-PKC $\zeta$  (Santa Cruz Biotechnology); anti-mouse Alexa Fluor 350, anti-mouse and anti-rat Alexa Fluor 488, anti-mouse and anti-hamster Alexa Fluor 568, anti-rat and anti-rabbit Alexa Fluor 647, and streptavidin-conjugated Alexa Fluor 647 (Molecular Probes). Hoechst 33258 (Invitrogen) was used to detect DNA. Stains were done for 1h at room temperature, and washes were done with blocking buffer.

For analysis of blasts, cells were selected based on large size by brightfield and the specific appearance of  $\beta$ -tubulin staining (Fig. S1). After identification of pre-mitotic and mitotic blasts, only then was the morphology of the other fluorescence channels revealed. In conjoined twin experiments, cells undergoing cytokinesis were first identified by pronounced cytoplasmic cleft by brightfield plus the presence of dual nuclei using Hoechst DNA stain. After identification of twins, only then was the morphology of the other fluorescence channels revealed. 20-30 Z stack sections were acquired using an Ultraview spinning disk confocal microscope (PerkinElmer Life Sciences). 3-dimensional Z stacks were converted into 2-dimensional images using IPLab for Macintosh and Adobe Photoshop.

For quantifying mitotic blasts, Volocity software was used to calculate the volume of 3-D pixels (voxels) containing the designated receptor fluorescence within each hemisphere. The two hemispheres were delineated using the pattern of  $\beta$ -tubulin fluorescence to define the poles of the mitotic spindle, with the equator bisecting the line connecting the two poles. Receptor enrichment at one hemisphere greater than 1.75-fold compared to the other hemisphere was considered polarized. P values were calculated using chi-square analysis. For conjoined twin experiments, pairs were scored for asymmetric segregation of staining between conjoined daughter cells. All images are depicted using pseudo-colors ("true" green channel occupied by CFSE fluorescence, not shown). In conjoined twin experiments, anti-tubulin staining was detected using Alexa Fluor 488, which could be resolved in the green channel due to its enhanced brightness relative to CFSE.

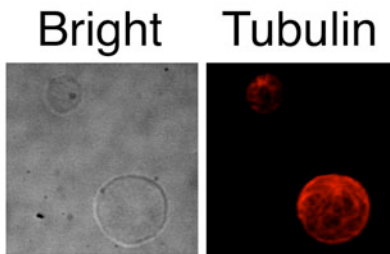


Figure S1. Selecting T cell blasts for microscopy. Undivided P14 transgenic CD8<sup>+</sup> T cells from gp-33-*L. monocytogenes*-infected wild-type recipients were harvested and analyzed by confocal microscopy. Blasts (lower right corner of each panel) could be readily identified by large cell size on brightfield (left panel) compared to the small size of an unactivated and/or early activated cell (upper left corner of each panel). Subsequent to blast identification, pre-mitotic cells could be identified by a single MTOC with  $\beta$ -tubulin staining (shown here; right panel). Mitotic blasts (not shown here; see Fig.1 and Fig.2 of the Research Article) were selected by their large size and the presence of two MTOCs.

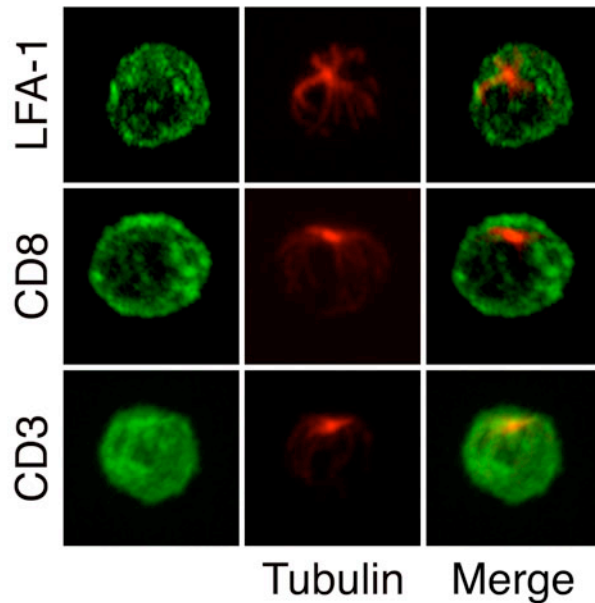


Figure S2. Diffuse staining of proteins in adoptively transferred naïve CD8<sup>+</sup> T cells. CFSE-labeled naïve P14 TCR transgenic CD8<sup>+</sup> T cells were transferred into naïve recipients. 32h after transfer, CFSE<sup>+</sup> cells (all undivided) were sorted from spleens of recipients, and examined by confocal microscopy after staining for  $\beta$ -tubulin (red) and either LFA-1, CD8, or CD3 (green).

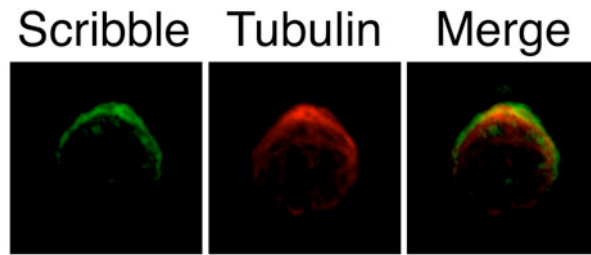


Figure S3. Scribble localizing to the putative immunological synapse in vivo. Cell-sorted, undivided P14 TCR transgenic T cells from gp33-*L. monocytogenes*-infected wild-type mice were examined by confocal microscopy after staining for Scribble (green) and  $\beta$ -tubulin (red). Because this localization is at variance with prior short-term, in vitro analysis (S2), we validated the present antibody by showing it specifically detects a Scribble-GFP fusion protein.

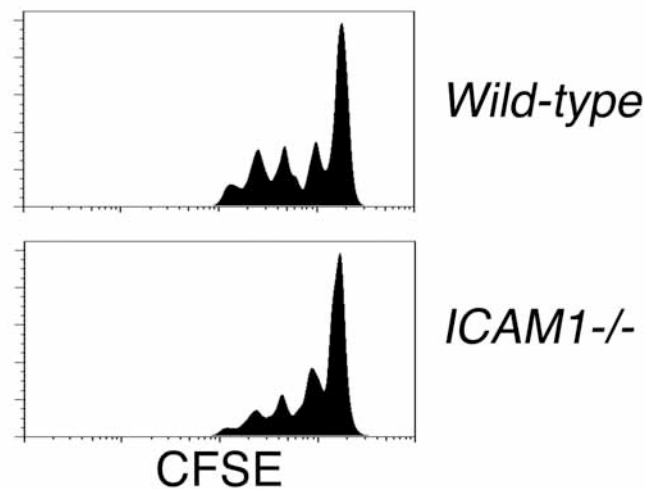


Figure S4. Efficient cell division in infected ICAM1-deficient recipients. P14 transgenic CD8<sup>+</sup> T cells from gp-33-*L. monocytogenes*-infected wild-type or *Icam1*<sup>-/-</sup> recipients were harvested 48h after infection and analyzed by flow cytometry to assess cell division based on CFSE dilution. Only CD8<sup>+</sup> electronically gated events are displayed.

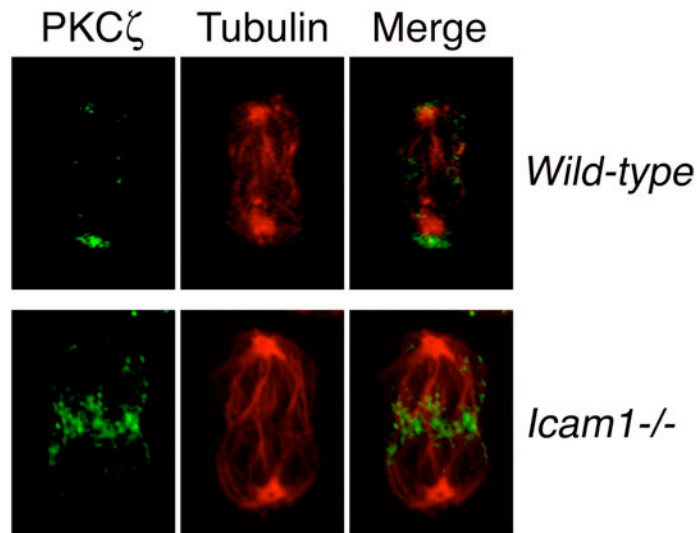


Figure S5. Disparity in protein inheritance of daughter CD8<sup>+</sup> T cells in vivo. P14 transgenic CD8<sup>+</sup> T cells from gp33-*L. monocytogenes*-infected wild-type or *Icam1*<sup>-/-</sup> recipients were harvested and the undivided fraction was sorted prior to antibody-staining for PKC $\zeta$  (green) and  $\beta$ -tubulin (red). Cells undergoing cytokinesis were identified by characteristic cleavage furrow by brightfield. Asymmetric segregation of PKC $\zeta$  in cells from wild-type recipient was distinct from localization at cleavage furrow observed in *Icam1*<sup>-/-</sup> recipient.

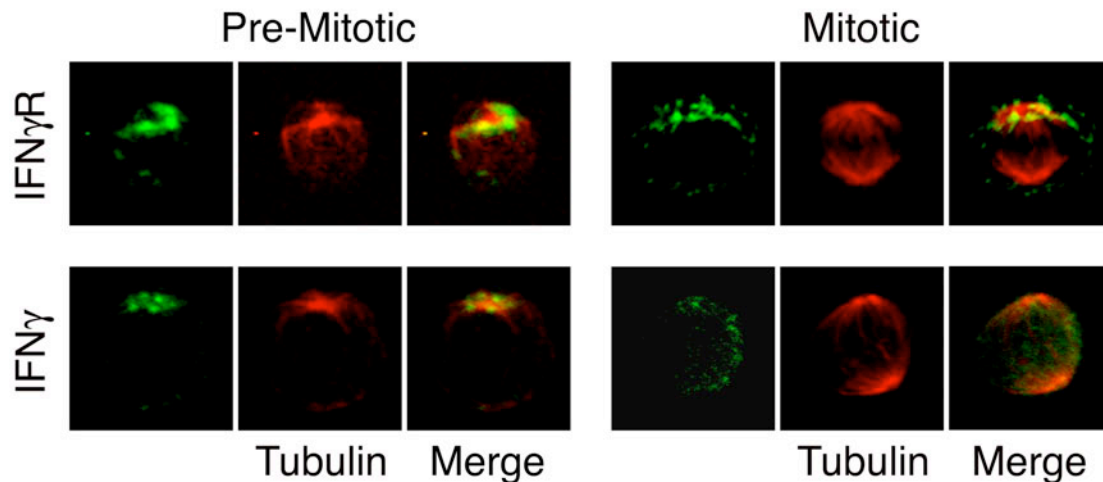


Figure S6. IFN $\gamma$ R and IFN $\gamma$  cytokine polarizing in CD8<sup>+</sup> T cells responding to infection. Undivided (parent) CD8<sup>+</sup> T cells from gp33-*L. monocytogenes*-infected mice were stained with antibodies against  $\beta$ -tubulin (red) and either IFN $\gamma$ R or IFN $\gamma$  (green). IFN $\gamma$ R was polarized at the putative immunological synapse of pre-mitotic blasts, and was asymmetrically partitioned relative to the spindle of mitotic cells. IFN $\gamma$  protein accumulated almost exclusively beneath the MTOC of pre-mitotic blasts, a pattern predictive of polarized secretion through the synapse (S3). In M-phase, however, IFN $\gamma$  staining had become diffuse, consistent with the known dispersion of the Golgi apparatus during mitosis.

Figure S7. T-bet mRNA induction in CD8<sup>+</sup> T cells promoted by autocrine IFN $\gamma$  signaling. Real-time RT-PCR was performed on purified CD8<sup>+</sup> T cells activated in vitro for 3h using immobilized anti-CD3 alone, with neutralizing anti-IFN $\gamma$  mAb, or with exogenously supplied rIFN $\gamma$ . Neutralizing mAbs against the cytokine significantly attenuated induction, and exogenously supplied recombinant IFN $\gamma$  only marginally augmented induction.

	Proximal	Distal
CD62L	53	222
CD69	208	24
CD43	371	123
CD44	775	206
CD25	421	21

Figure S8. Disparity in phenotypic markers of first daughter T cells responding to infection. Initial daughter CD8<sup>+</sup> T cells from gp33-*L. monocytogenes*-infected mice were analyzed by flow cytometry with antibodies against CD8 and CD62L, CD69, CD43, CD25, or CD44 (Fig. 5A of the Research Article). Mean fluorescence intensity of gated proximal and distal daughters is presented in tabulated form.

### Supplemental References

- S1. Q. Wang *et al.*, *J Immunol* **167**, 4311 (2001).
- S2. M. J. Ludford-Menting *et al.*, *Immunity* **22**, 737 (2005).
- S3. M. Huse, B. F. Lillemeier, M. S. Kuhns, D. S. Chen, M. M. Davis, *Nature Immunology* **7**, 247 (2006).